OPTIMIZING THE ENERGY PRODUCTION FOR A PHOTOVOLTAIC THERMAL WATER SYSTEM

by

Khader M.J. Alsayegh

A Thesis presented to the Faculty of the
American University of Sharjah
College of Engineering
In Partial Fulfilment
of the Requirements
for the Degree of

Master of Science in
Mechanical Engineering

Sharjah, United Arab Emirates

May 2022

Declaration of Authorship

I declare that this thesis my own work and, to the best of my knowledge and belief, it does not contain material published or written by a third party, except where permission has been obtained and/or appropriately cited through full and accurate referencing.

Signed **Khader Alsayegh**

Date **9/5/2022**

Approval Signatures

We, the undersigned, approve the Master's Thesis of Khader M.J. Alsayegh

Thesis Title: Optimizing the Energy Production for a Photovoltaic Thermal (PVT) Water System

Date of Defence: 9/5/2022

Name, Title and Affiliation	**Signature**
Dr. Mohamed O. Hamdan Professor, Department of Mechanical Engineering Thesis Advisor	
Dr. Mehmet F. Orhan Associate Professor, Department of Mechanical Engineering Thesis Co-Advisor	
Dr. Bassam A. Abu-Nabah Associate Professor, Department of Mechanical Engineering Thesis Committee Member	
Dr. Mahmoud Awad Associate Professor, Department of Industrial Engineering Thesis Committee Member	
Dr. Mamoun F. Abdel-Hafez Head Department of Mechanical Engineering	
Dr. Lotfi Romdhane Associate Dean for Graduate Affairs and Research College of Engineering	
Dr. Fadi Aloul Dean College of Engineering	
Dr. Mohamed El-Tarhuni Vice Provost for Research and Graduate Studies Office of Research and Graduate Studies	

Acknowledgements

I would like to thank my advisors Dr. Mohamed Omar Hamdan and Dr. Mehmet Fatih Orhan for guiding me through the research stages. Their insight, knowledge, patience, and persuasion propelled me to work hard and become a better researcher. I appreciate the long hours and the sincere efforts that they spent in helping me through this research topic.

I also wish to thank the members of the examination committee, Dr. Bassam Abdel Jaber Abu-Nabah and Dr. Mahmoud Awad, for the constructive discussion and thoughtful advice.

I would like to thank Eng. Munther Yacoub Alsayegh for his invaluable suggestions and continuous support. His knowledge of the various engineering systems and devices helped me in running my experiment. Through his motivation, I became a better engineer and researcher.

I would like to express my gratitude to the American University of Sharjah for supporting my research work and offering me a graduate assistantship. The graduate assistantship allowed me to gain invaluable research and teaching skills.

Dedication

To my family…

Abstract

The maximum exploitation of solar energy can be achieved through the optimization of a photo-voltaic thermal (PVT) system. In the PVT system, the (PV) module is cooled down by a water-based thermal collector, and as a result, electricity and hot water are produced. A novel zero-dimensional model is proposed to assess and optimize the performance of such a PVT system. The zero-dimensional model does not rely on spatial resolution or time-dependent variables. The model consists of thermodynamic relations that analyze the energy and the exergy of the PVT system. The validation of the model is performed by comparing its prediction parameters to the parameters collected experimentally from an in-house PVT system. The in-house PVT system consists of a polycrystalline PV module attached to a double series-parallel serpentine thermal collector. The zero-dimensional model predicts the difference between inlet and outlet water temperature as well as the PV surface temperature with an average error of $0.13\,℃$ and $1.80\,℃$, respectively. Using the zero-dimensional model, the optimization of the PVT performance is achieved by choosing the optimal mass flow rate and inlet temperature for the system. For the experimental setup, a mass flow rate of $0.001\,kg/s$ and an inlet temperature close to a relatively low ambient temperature provided the highest overall second law efficiency of 15.2%. The PVT system performs the best in regions with relatively low ambient temperature yet high solar radiation.

Keywords: Photovoltaic-Thermal System (PVT); Thermal Collector (TC); zero-dimensional model; energy analysis; exergy analysis

Table of Contents

List of Figures

List of Tables

List of Abbreviations

A_{PV}	PV area (m^2)
D_h	Hydraulic diameter (m)
$\dot{E}$	Electrical energy produced by the PV (W)
h_w	Heat transfer coefficient of the moving air ($W/m^2.K$)
G	Total irradiance (W/m^2)
k_w	Thermal conductivity of water (W/m.K)
$\dot{m}$	Mass flow rate (Kg/s)
$\dot{Q}$	Rate of heat transfer (W)
$\dot{Q}_u$	Useful heat gain (W)
$\dot{Q}_{conv}$	Rate of heat transfer by forced convection (W)
$\dot{Q}_{rad}$	Rate of heat transfer by radiation (W)
T_a	Ambient temperature (K)
T_i	Inlet temperature (K)
T_s	Surface temperature (K)
T_{sun}	Sun's temperature (K)
T_o	Outlet temperature (K)
ΔT_{LMT}	Log mean temperature
$U_{overall}$	Overall convection coefficient of the PV ($W/m^2.K$)
v	Speed of wind (m/s)
$\dot{X}_{solar,in}$	Rate of solar exergy that reaches the Earth (W)
$\dot{X}_{th}$	Rate of recovered thermal exergy (W)

$\dot{X}_{ele}$	Rate of recovered electrical exergy (W)

Constants

β	Temperature coefficient (K^{-1})	0.0045
σ	Stefan Boltzmann constant ($W/m^2.K^4$)	$5.67*10^{-8}$
η_{ref}	Reference efficiency	0.139
ε_{PVT}	Thermal emissivity of the PVT	0.9

Abbreviations

PV	Photovoltaic cell
TC	Thermal Collector
PVT	Photovoltaic Thermal System

Greek Letters

ρ	Density (kg/m^3)
υ	Kinematic viscosity of water (m^2/s)
η	Overall efficiency of the PVT system
η_{ele}	Electrical efficiency of the PVT system
η_{th}	Thermal efficiency of the PVT system
η_{II}	Overall second law efficiency of the PVT system
$\eta_{\mathrm{II},ele}$	Second law efficiency of the PV
$\eta_{\mathrm{II},th}$	Second law efficiency of the TC

Chapter 1. Introduction

1.1. Introduction

In this chapter, a short introduction about PVT systems is provided. The working principles, the importance of PVT systems, and the need to optimize the performance of water-based PVT systems are highlighted. Then, we display the thesis contribution to optimizing the performance of water-based PVT systems. Finally, the organization of the thesis is presented.

1.2. Overview

The increase in energy demand propels countries to diversify their energy sources. Currently, the world mainly relies on fossil fuels, such as coal, oil, and natural gas, to satisfy the energy needs. The depletion of fossil fuels as well as their harmful emissions forces the world to seek sustainable renewable energy sources. For instance, the countries that receive high solar irradiance, such as the Gulf Cooperation Council (GCC) countries, are shifting their interest towards solar energy [1]. Typically, solar energy is harvested by photovoltaic (PV) panels and thermal collectors. PV panels convert solar energy directly to electricity whereas thermal collectors convert solar energy to thermal energy. The hybrid photovoltaic-thermal (PVT) system combines the production of electrical and thermal energy from solar energy [2]. The PVT system consists of a PV module attached to a thermal collector. The PVT system is an interesting prospect as it optimizes the exploitation of solar energy, where some of the unexploited solar energy by the PV module is utilized by the thermal collector. The thermal collector produces hot water that could be used in domestic applications while simultaneously cooling down the PV panel. Radziemska [3] has shown that the increase in the temperature of the PV frontal surface beyond the room temperature linearly decreases the electrical efficiency. Fudholi et. al [4] has reported that for every 10 °C increase in the PV temperature beyond the room temperature, the electrical efficiency decreases by 5%. The thermal collector carries away the heat from the PV panel leading to an increase in its electrical efficiency, which improves the exploitation of the solar energy. Han et. al [5] has proved that the utilization of PVT systems instead of stand-alone PV modules in countries that receive high intensity of solar radiation is justifiable as the PVT systems have relatively high electrical efficiency.

The ability of the PVT system to generate both electricity and hot water has motivated researchers to devise optimized designs of PVT systems. The relevant literature includes various designs of thermal collectors that optimize the performance of PVT systems. Also, mathematical models such as PVT 1-D model, PVT 2D-model, and PVT 3-D model that predict the effect of weather conditions and operational parameters on the performance of the PVT system are present in literature. The proposed zero-dimensional model predicts the performance of the PVT system regardless of the design of its thermal collector and allows researchers to study the effect of different parameters on the PVT performance by utilizing simple, thermodynamic relations.

1.3. Thesis Objectives

In line with the UAE's clean-energy vision of 2050, the current study focus is aiming to optimize the performance of photovoltaic thermal systems [6]. This thesis aims to provide a zero-dimensional mathematical model that predicts the performance of any PVT system, regardless of its size, materials, or design. The model will be able to quantify the overall first-law efficiency of the system as well as its second law efficiency. The results of the model are compared with the results derived from an in-house experimental setup. The experimental setup consists of a heat sink that has water flowing through its pipes which is connected directly to a PV module.

1.4. Research Contribution

The contributions of this research work can be summarized as follows:

- Validate the zero-dimensional PVT model by comparing its predictions of the PVT performance to the collected data from the in-house PVT system. The zero-dimensional model predicts the difference between inlet and outlet water temperature as well as the PV surface temperature with an average error of 0.13 ℃ and 1.80 ℃, respectively.
- Utilize the zero-dimensional model to conduct parametric studies to understand the effect of the ambient temperature, the inlet water temperature, the mass flow, the solar irradiance, and the wind speed on the performance of the PVT system
- Prove that the optimal performance of the PVT system is achieved in countries that have cold climates yet receive long hours of intense solar radiation

1.5. Thesis Organization

The rest of the thesis is organized as follows: Chapter 2 provides background about PVT systems and the principles of its operation. Moreover, the experimental and the numerical research related to the water-based PVT systems is discussed. In Chapter 3, the equations that make up the zero-dimensional model along with the assumptions are showcased. Chapter 4 portrays the in-house experimental setup and the design and fabrication processes of the thermal collector. The validation of the zero-dimensional model is outlined in Chapter 5. Also, an in-depth parametric study that highlights the effects of mass flowrate, inlet temperature, wind speed, solar irradiance, and ambient temperature on the performance of the water-based PVT system is performed in Chapter 5. Finally, Chapter 6 summarizes the thesis and discusses ways to extend on this work.

Chapter 2. Background and Literature Review

In this chapter, we discuss the principle of PVT systems and their importance. Then, the optimized experimental designs of water-based PVT systems are showcased. This is followed by a review of various mathematical models that predict the performance of PVT systems.

2.1. Basics of PVT System

The PVT system maximizes the exploitation of the solar energy by transforming solar irradiance to electricity and thermal energy. The PVT system mainly consists of a PV module and a thermal collector, as seen in Figure 2-1. Fundamentally, the thermal collector is a heat sink in which the water flows and cools down the PV unit. Through the PV module, electricity is produced. However, the electrical efficiency of the PV module deteriorates as its temperature increases. The thermal collector cools down the PV module while simultaneously yielding hot water. The PVT system is a valid solution to the electricity needs and hot water scarcity in rural areas [7].

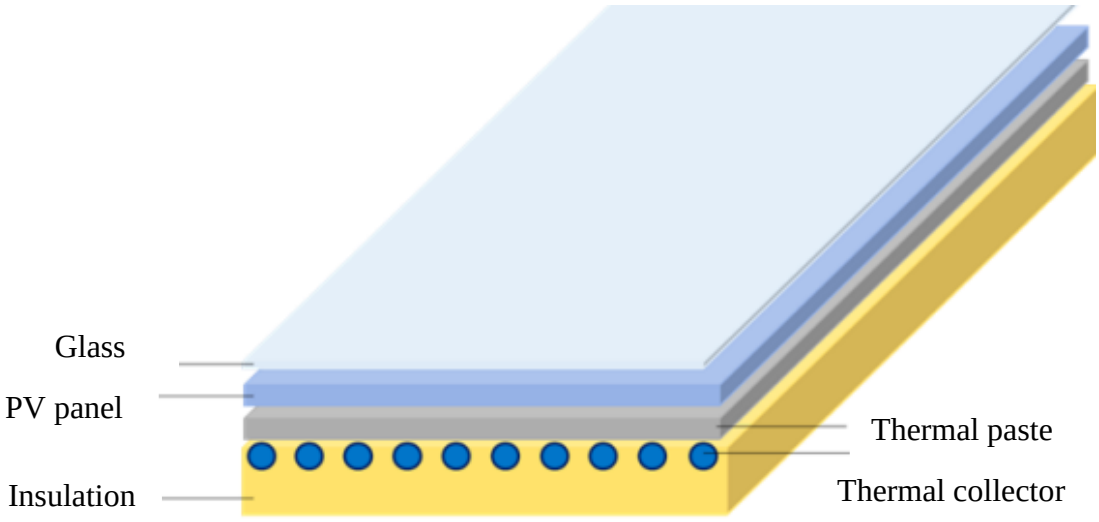

Figure 2-1: Basic PVT schematic [5]

In general, PVT systems are categorized based on their cooling method. Active cooling requires the forced circulation of a fluid by means of a pump or a fan, whereas passive cooling relies on the natural circulation of a fluid. While many complex cooling technologies are emerging, air- and water-based cooling systems remain the most mature and widely used technologies [8]. Air-based cooling includes passive cooling techniques such as the employment of fins on the backside of the PV panel to facilitate

convection [9], and active cooling techniques such as forced airflow in ducts that are placed beneath the PV module [10]. Water-based cooling is mainly achieved through active systems such as water spraying and forced water circulation. Forced water circulation is done by pumping water in pipes that are attached to the backside of the PV panel to absorb the excess heat from the panel. Forced water circulation is relatively easy to implement and effective in decreasing the temperature of a PV panel [8].

2.1.1. Creating electricity

Capturing solar energy and transforming it into electricity is currently achieved through the usage of silicon solar cells and PV modules. The creation of electricity in the semiconductor-based PV modules is made possible through the implementation of the p-n junction. Each side of the Silicon, a semiconductor, is doped with different dopants. For instance, the p-side is doped with Boron making it relatively conductive whereas the n-side is doped with Phosphorus making it conductive. The region between the two sides is non-conductive. Silicon has electrons in two bands, a low valence band, and a high conduction band. As the incoming photons from the Sun are absorbed by the Silicon PV module, the movement of electrons and holes creates electricity. To explain, for the electrons in the low-valence band to get excited and move towards the conduction band, band-gap energy should be supplied through photons or phonons. The bandgap energy for Silicon is 1.1 eV [5]. If the absorbed photons from the sunlight have long wavelengths and energy less than the band-gap energy, the electrons will not get excited and the energy from the photons will be dissipated as heat. If the absorbed photons from the sunlight have shorter wavelengths and high energy, electrons will leap to the conduction band but the excess energy from the photons will be dissipated into heat. The motion of the electrons is always towards the p-side whereas the motion of the holes is in the opposite direction. This creates a voltage difference between the two sides and electricity is generated accordingly [6]. For this proposal, only Silicon solar cells will be considered since around 80% of the utilized solar cells are either monocrystalline Silicon cells or polycrystalline Silicon cells [7].

2.1.2. Temperature limitation on the PV performance

As the temperature of the PV panel increases, the open-circuit voltage decreases. The reduction in the open-circuit voltage implies a decrease in power generation and electrical efficiency. Radziemka concluded that increasing the temperature from 26

degrees Celsius to 60 degrees Celsius would cause around a 40% drop in electrical efficiency [11]. An increase in the temperature of the PV module increases the vibrations of the thermal lattice leading to the scattering of the electrons. This scattering of electrons implies that more collisions will occur, and more energy will be lost. Also, the increase in vibrations decreases the mobility of holes which in turn weakens the built-in voltage at the p-n junction [11]. Combining a PV module to a thermal collector controls the temperature of the PV and bolsters the overall efficiency. On average, combining the PV module with a thermal collector increases the PV electrical efficiency by 1.6% whereas the thermal efficiency of the thermal collector ranges from 29.44% to 44.84% [12].

2.1.3. Effect of glazing on the performance of the PVT system

The temperature of the PV panel is dependent on its glazing. Unglazed PV panel are more likely to have low surface temperature and high electrical efficiency. Kim and Kim [13] studied the relation between the PV surface temperature and electrical efficiency by comparing the performance of an unglazed PVT system with a glazed PVT system. Under the same weather conditions, the relatively hot glazed PVT system had 1.4% lower electrical efficiency and 14% higher thermal efficiency than the relatively cold unglazed PVT system. Fujisawa and Tani [14] performed energy and exergy analysis on a glazed PV module, an unglazed PVT system, and a glazed PVT system. The glazed PVT system had the highest overall efficiency, followed by the unglazed PVT system and the glazed PV module. However, the unglazed PVT system had the highest overall second law efficiency followed by the PV module and the unglazed PVT system. Similarly, Kazemian et. al [15] proved that the unglazed PVT system has a higher electrical exergy than the glazed PVT system. Tripanagnostopoulos et. al [16] concluded that the implementation of glazing in a PVT system is only useful in increasing the thermal gain. The study showed that the glazed PVT system could maximize the thermal efficiency by 30% but the electrical efficiency would be decreased due to the optical losses. It was recommended to use diffusion reflectors along with PVT system to maximize both the thermal efficiency and electrical efficiency.

2.1.4. Advantages and disadvantages of a PVT system

PVT system is one whose constituents are a Photovoltaic module, a thermal collector, connecting cables, and an inverter. If it is water-based, tanks that contain the water volume are required. If it is an active system, a pump or fan is needed to forcibly circulate the fluid. With the constituents of a PVT system in mind, it is concluded that the major advantage of this system is its simplicity. Other advantages of PVT systems include [17]:

- Working in noiseless environments
- Producing no toxic waste or radioactive waste, making it a clean technology
- Having a life span expectation of 20 to 30 years
- Performing at high levels with high reliability
- Requiring fewer maintenance sessions

While the advantages are prevalent, some disadvantages exist such as:

- Uniform cooling of PV panels is difficult to achieve meaning that the absorber designs require improvements.
- Production and installation cost is high

2.2. Optimization of PVT Performance

Efforts to optimize the performance of PVT systems have intensified in the last two decades. PVT optimization entails increasing the electricity generation as well as the hot water generation while keeping the rest of the parameters the same. Experimentally, researchers have designed and fabricated various designs of thermal collectors that increase the rate heat transfer from the PV module to the thermal collector. Numerically, PVT designs were analyzed through finite element analysis software. Most importantly, the operating and geometric variables of the PVT system were optimized using mathematical models that mimic the PVT performance.

2.2.1. Experimental and numerical design of thermal collectors

Many studies have been conducted to optimize and model the performance of a water-based PVT system. Experimental studies mainly focused on the design of thermal collectors.

Yu [18] tested two designs of thermal collectors, namely a harp-channel and a grid-channel absorbers, shown in Figure 2-3. In comparison to the harp-channel absorber, the grid-channel absorber had a 10% increase in its thermal efficiency that yields a 2% increase in the overall electrical efficiency of the PVT system.

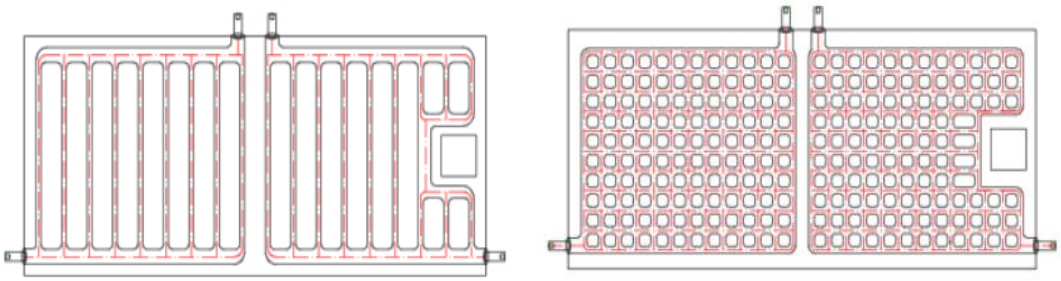

(a) (b)

Figure 2-3: (a) Harp-channel thermal collector (b) Grid-channel thermal collector [18]

Verma et al. [19] compared a spiral collector to a conventional parallel tubes collector. The spiral tube collector increases the thermal efficiency of a conventional tube collector by 21.94%. This increase in the thermal efficiency is related to the improved rate of heat transfer between water and the tubes. The centripetal action in the spiral flow causes the water to flow under the influence of centripetal forces leading to an improved rate of heat transfer.

Col et al. [20] investigated the performance of standard flat plate collector and roll-bond flat plate collector. The roll-bond flat plate collector provided higher efficiency curve than the standard collector. The study concluded that applying a heat-insulative coating to the thermal collector enhances its performance.

Visa et al. [21] analyzed the performance of thermal collectors with copper or aluminum substrates. The researchers concluded that varying the substrate of the absorber plate has minimal influence on the performance of the PVT as the aluminum thermal collector had only 1% increase in the overall efficiency.

Siddiqui et al. [22] showcased 14 thermal collector designs with different intake manifolds. The 14 designs could be categorized as either parallel-flow or series-parallel double serpentine heat sinks. Table 2-1 categorizes the 14 designs on geometric basic and lists the operating variables of these designs

Table 2-1: Analysis of the 14 thermal collector designs [22]

Design	**Channel Type**	**Number of Channels**	T_o (K)	$T_{s,avg}$ (K)	$T_{s,max}$ (K)	$T_{s,min}$ (K)	**Pressure Drop (Pa)**	ΔT_s (K)	$\frac{\dot{Q}}{\dot{W}_{pump}}$
1	Parallel	10	300.1	302.1	305.7	298.4	434.8	7.30	21241
2	Parallel	20	300.1	302.0	305.8	298.4	431.8	7.40	21389
3	Wider Header	10	300.1	301.6	304.7	298.4	250.7	6.30	36840
4	Tapered Header	10	300.1	302.0	305.6	298.4	377.9	7.20	24440
5	Tapered Header	10	300.1	302.0	305.6	298.4	373.2	7.20	24748
6	Tapered Header	10	300.1	301.9	305.1	298.7	336.7	6.40	27430
7	Tapered Header	10	300.1	301.5	304.0	298.7	178.1	5.30	51858
8	Tapered Header	10	300.1	301.7	304.1	298.6	358.2	5.50	25784
9	Tapered Header	10	300.1	301.4	303.5	298.7	168.1	4.80	54943
10	Centered Inlet and Outlet	10	300.1	301.5	304.0	298.6	158.9	5.40	58124
11	Centered Inlet and Outlet	10	300.1	301.5	303.7	298.6	158.6	5.10	58234
12	Centered Inlet and Outlet	10	300.1	301.5	303.3	298.6	159.4	4.70	57942
13	Series-Parallel	10	300.1	299.8	300.6	298.4	899.3	2.20	10270
14	Series-Parallel	18	300.1	299.5	300.2	298.4	5028.0	1.80	1836

The double series-parallel serpentine heat sinks, designs 13 and 14, had a low surface temperature and low non-uniformity in the temperature distribution, whereas the parallel flow heat sinks had a high heat transfer rate to pumping power ratio. Figure 2-

3 shows an example of a parallel flow thermal collector and a double series-parallel serpentine thermal collector.

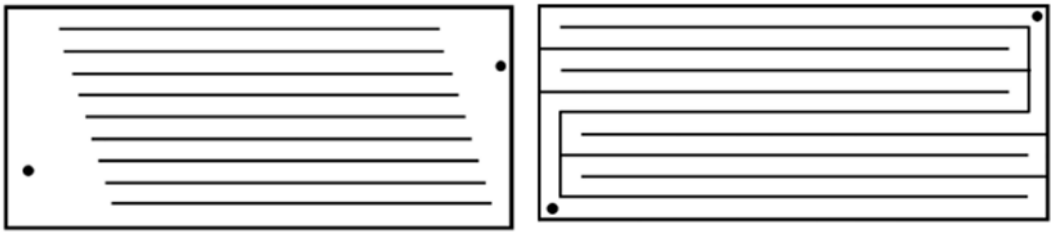

(a) (b)

Figure 2-4: (a) Design 9 (b) Design 13 [22]

Kazem et al. [23] experimentally developed three PVT systems and recorded their electrical efficiencies. The three PVT systems were direct flow PVT, spiral flow PVT, and web flow PVT, as seen in Figure 2-5. The spiral flow PVT resulted in the lowest PV surface temperature and the highest overall efficiency. The study showed that the spiral flow PVT system had an electrical efficiency that is 2% and 0.6% higher than that of the direct flow PVT system and the web flow PVT system, respectively.

(a) (b) (c)

Figure 2-5: (a) Direct flow PVT (b) Spiral flow PVT (c) Web flow PVT [23]

Ibrahim et al. [24] studied the effect of ambient temperature on a the performance of a water-based PVT system whose thermal collector is a spiral flow absorber. The study concluded that the overall efficiency of the PVT system increases as the ambient temperature remains low. The study suggested the usage of cold water at the inlet of the thermal collector to boost the electrical efficiency of the system.

Pang et al. [25] carried out a study to optimize the performance of a water-based PVT system by increasing the contact surface between the PV module and the thermal collector. The study showed that a roll-bound aluminum collector that is combined with

the PV module through an advanced thermal fusion welding technology provide the highest overall efficiency.

In a numerical study, Ibrahim et al. [26] designed 7 thermal collectors and studied the effect of the spacing between the tubes on the PVT performance. Figure 2-6 shows the thermal collectors with the highest number of tubes, namely the spiral flow, the parallel-serpentine flow, and the modified serpentine-parallel flow thermal collectors, which had the highest overall efficiencies of 68%, 60%, and 58%, respectively.

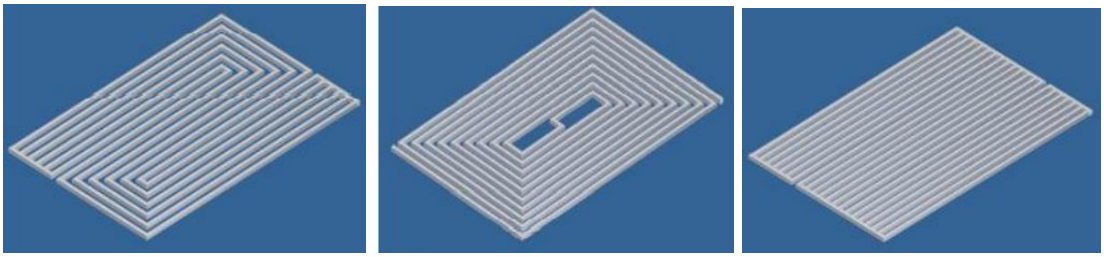

(a) (b) (c)

Figure 2-6: Designs of thermal collectors: (a) Spiral flow (b) Parallel-serpentine flow (c) Modified serpentine-parallel flow [26]

Fayaz et al. [27] conducted a simulation-based study to observe the effect of pipe diameter on the overall efficiency of the PVT system. The study proved that increasing the inner pipe diameter decreases the thermal efficiency of the thermal collector. The highest thermal efficiency of 74% was recorded at the lowest pipe diameter of 3.5 mm whereas the lowest thermal efficiency of 62% was recorded at the highest pipe diameter of 15.5 mm.

2.2.2. Mathematical models of PVT systems

Numerical studies have mainly focused on optimizing the performance of the PVT system by varying parameters.

Zondag et al. [28] provided four mathematical models and compared their performance to that of a water-based non-optimized serpentine PVT system. The four mathematical models that were tested are steady 1D, 2D and 3D models and a dynamic 3D model. The study showed that both the dynamic and the steady 3D models have the ability to simulate the PVT while accounting for the fluctuating solar irradiance. The steady 2D model has dealt with the PVT system as layers, whereas the steady 1D model strongly depends on the tube spacing to tube diameter ratio. It has been concluded that the steady 1D provides satisfactory results as the deviation of results between 1D and 2D models

and 1D and 3D models is 1% and 3%, respectively. Table 2-2 compares the computation time of the proposed models by Zondag.

Table 2-2: Calculation time of Zondag's models [28]

Model type	**Calculation time**	
	Efficiency curve	**Hourly yield**
1D steady model	0.27 s	0.05s
2D steady model	8.35 s	1.67s
3D steady model	229.31 s	45.86 s
3D dynamic model	-	2.5 h

Pierrick et al. [29] proposed a dynamic 3D finite element water-based PVT model. The dynamic 3D model has shown an acceptable accuracy in predicting the outlet water temperature. The study reported that the dynamic 3D model is best utilized to optimize the geometry of the thermal collector at the cost of long computational time.

Guarracino et al. [30] discussed a dynamic 3D finite volume-based model of water-based PVT that estimates the temperature distribution over the surface of the PVT system, which allows the computation of thermal and electrical efficiencies. The study showed that the electrical efficiency drops by 4% when the PV panel overheats, while the introduction of a thermal collector allows the panel to operate over its nominal electrical efficiency.

Soliman et al. [31] developed a steady 3D finite-volume model that implements energy balance on the different layers of the PVT system, while using constant thermo-physical properties. The steady 3D model has predicted the cell temperature to decrease by $15\ ℃$ when a geometrically optimized thermal collector is used.

Sami [32] presented a dynamic 2D finite difference-based model that discretizes the PVT system into thermal elements. The iterative model has underestimated the cell temperature by $1-2\ ℃$.

Dubey and Tiwari [33] validated a dynamic 2D finite difference-model with the experimental data that is collected from the PVT system. The model provided accurate results, in which the experimental and theoretical outlet temperature had a correlation coefficient of 0.9996% and root mean square percent deviation of 1.37%, respectively.

Ji et al. [34] proposed a dynamic 2D model that predicts the performance of a PVT system that has a serpentine thermal collector. The dynamic 2D model is based on implicit finite difference relations that are solved at the discretized scheme as shown Figure 2-7. The model provides satisfactory outcome in which the highest deviation of 8% happens when predicting PV efficiency.

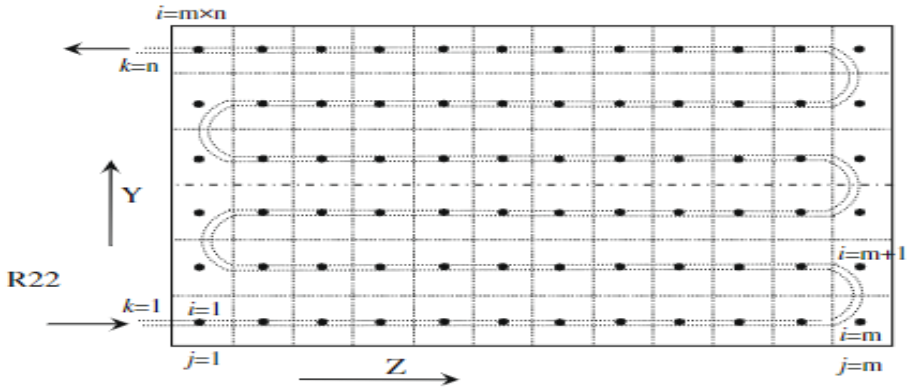

Figure 2-7: Discretization of collector plate in Ji's model [34]

Tiwari and Sodha [35] adopted a dynamic 1D model to predict the performance of the water-based PVT system. The dynamic 1D model considered time-dependent variables while dealing with the layers of the PVT system, the convective, and radiative effects as thermal resistances. Figure 2-8 clearly shows the setup of the thermal resistances in the proposed model. The model provided fair agreement between experimental and numerical data, in which the experimental and the theoretical cell temperatures had a correlation coefficient and a root mean square percent deviation of 0.98% and 7.22%, respectively.

Bahaidarah et. al [36] compared the performance of the water-based PVT system to the performance of a stand-alone PV system using a 1D dynamic model. The 1D transient model deals with the PVT layers and the PV layers as thermal resistances. The study showed that the PVT system had an increase of 9% in the electrical efficiency when compared to the standalone PV system.

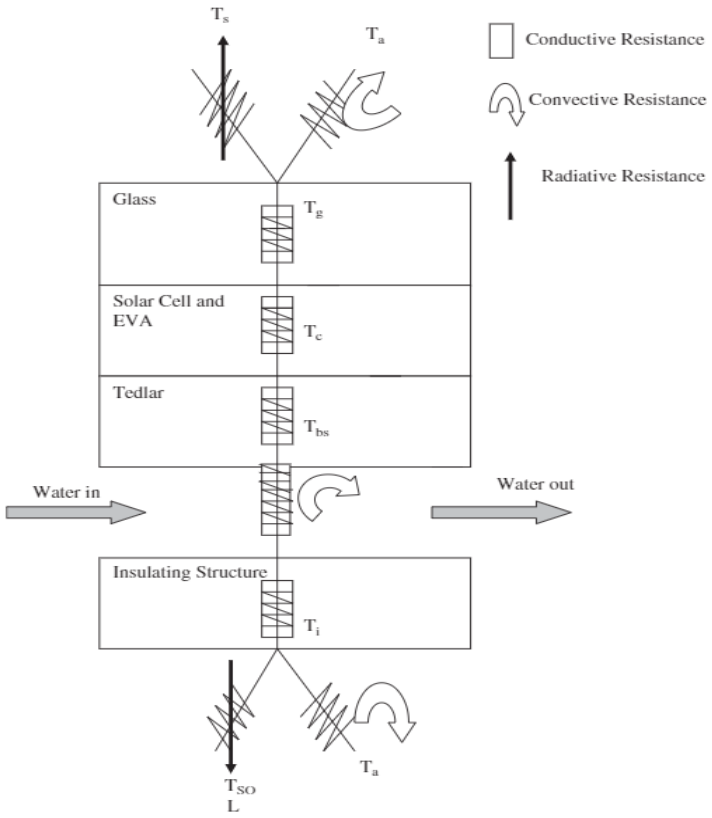

Figure 2-8: Thermal resistance circuit diagram for the PVT system [35]

Evola and Marletta [37] investigated the effect of inlet temperature on the performance of a water-based PVT system using a steady 1D model that incorporates both the first and second laws of thermodynamics. The steady 1D model proved that operating at a low inlet water temperature provides a high thermal efficiency of 50%, but a very low second law thermal efficiency of 4%. The study has concluded that optimized PVT performance is achieved when the inlet water temperature is in the range of 30 to 35 ℃.

Abdulalah et. al [38] studied the relation between the mass flowrate and the performance of the water-based PVT system using a steady 1D model. The model predicted that the electrical efficiency increases with increasing mass flow rate. Also, the model was validated by comparing its results with experimental data that is collected from a PVT system whose thermal collector is a dual oscillating absorber. The mathematical model had an error of 1.4 ℃ in predicting the PV surface temperature. A summary of these studies [27-37] is presented in Table 2-3, which summarizes the input parameters of each numerical model to assess and optimize the performance of the PVT system properly.

Table 2-3: Comparison between the mathematical models of the PVT system

Model Type	**Thermo-physical properties**	**Geometry of the PVT system**	**Weather conditions**	**Reference**
Dynamic 3D model	Time-dependent	Detailed 3D geometry	Fluctuating	[28],[29], [30]
Steady 3D model	Fixed at average temperature	Detailed 3D geometry	Constant	[28], [31]
Dynamic 2D model	Time-dependent	Length and thickness of PV and TC	Fluctuating	[32], [33], [34]
Steady 2D model	Fixed at average temperature	Length and thickness of PV and TC	Constant	[28]
Dynamic 1D model	Time-dependent	Thickness of absorption pipes	Fluctuating	[35], [36]
Steady 1D model	Fixed at average temperature	Thickness of absorption pipes	Constant	[28], [37], [38]

Chapter 3. Methodology

The literature review and Table 2 indicate that there has been no/little zero-dimensional model, which can allow quick simple optimization of PVT systems. Therefore, to fill this gap and help ongoing efforts of improving PVT applications, the objective of this study is to assess and optimize the performance of a photovoltaic-thermal (PVT) system via a novel zero-dimensional model that does not rely on spatial resolution or time-dependent variables. The zero-dimensional model uses thermodynamic relations that yield energy and exergy analyses of the PVT system.

3.1. Problem Formulation

The zero-dimensional mathematical model is proposed to predict the behavior of the PVT system. The mathematical model is validated against an in-house experimental PVT system. The in-house experimental setup consists of a PV module that is cooled via a double serpentine series-parallel thermal collector attached to its backside. Water is pumped inside the thermal collector. Using the validated model, a parametric study is conducted to optimize various design and operation parameters such as mass flow rates, inlet temperature, solar irradiance, wind speed and improve the overall performance of the system.

3.2. Zero-dimensional Mathematical Model

The zero-dimensional thermodynamic model is independent of space and time. This model assesses the performance of the PVT system using energy and exergy balances with the knowledge of the working fluid thermal properties, the fluid inlet conditions, the ambient conditions, and the surface temperatures of the PV and thermal collector. The following assumptions are used in the proposed zero-dimensional model:

- The thermal and physical properties of the working fluid and the PVT system are independent of temperature [39].
- Negligible heat loss occurs from the back and the sides of the thermal collector.
- Wind speed is independent of position.
- There is no shading and soiling on the PVT system.
- The system is in a quasi-equilibrium condition.

- Diffused radiation does not affect the PVT system [40].
- The temperature of the sun is $T_{\text{sun}} = 6000$ K [41].
- The thermal collector overall heat transfer coefficient, U_{avg}, is independent of the mass flow rate.
- Water is used as the working fluid.

The relevant modelling parameters are presented in Table 3-1.

Table 3-1: PVT physical and thermal properties

Parameter	**Value**
Surface area of PVT system (A_{PV})	0.358 m^2
Hydraulic diameter of pipes (D_h)	0.09 m
Specific heat capacity of water (C_p)	4186 J/kg. K
Temperature coefficient (β)	0.0045 1/K
Thermal emissivity of the PV (ε_{PV})	0.9
Reference efficiency of PV (η_{ref})	0.139

The overall PVT efficiency (η) is a combination of the electrical efficiency of PV (η_{ele}) and the thermal efficiency of the thermal collector (η_{th})

$$\eta = \eta_{th} + \eta_{ele} \tag{1}$$

Electrical efficiency is a measure of the amount of solar energy (G) converted to electrical energy ($\dot{W}_e$) as the sun rays hit the surface area of the PV cell (A_{PV}).

$$\eta_{ele} = \frac{\dot{W}_e}{G A_{PV}} \tag{2a}$$

The electrical efficiency depends on the PV surface temperature (T_s). The increase in surface temperature substantially decreases the open-source voltage, slightly increases the short circuit current, and decreases the electrical efficiency [42]. The electrical efficiency depends on parameters provided by the PV manufacturer, such as the reference efficiency (η_{ref}), reference temperature (T_{ref}), and temperature coefficient (β).

$$\eta_{ele} = \eta_{ref}[1 - \beta(T_s - T_{ref})] \tag{2b}$$

Thermal efficiency is a measure of the amount of solar energy converted to thermal energy ($\dot{Q}_u$). This parameter depends on the design of the thermal collector and the weather conditions.

$$\eta_{th} = \frac{\dot{Q}_u}{GA_{PV}} \tag{2c}$$

The amount of heat absorbed by the thermal collector is related to the increase of the sensible energy of the working fluid. The mass flow rate ($\dot{m}$), the specific heat capacity of water (c_p), the inlet (T_i) and the outlet (T_o) water temperatures are used in the formulation.

$$Q_u = \dot{m}c_p[T_o - T_i] \tag{3}$$

The heat transfer absorbed by the thermal collector is driven by internal forced convection heat transfer mechanism. The heat transfer absorbed depends on of the overall heat transfer coefficient ($U_{overall}$) and the log mean temperature difference (ΔT_{LMT}) as shown in Eq. (4) [43].

$$\dot{Q}_u = U_{overall}A_{PV}\Delta T_{LMT} \tag{4}$$

The overall heat transfer coefficient is experimentally deduced. The log mean temperature difference is calculated as a function of PV surface temperature, inlet and outlet water temperatures.

$$\Delta T_{LMT} = \frac{T_i - T_o}{\ln\left(\frac{T_s - T_o}{T_s - T_i}\right)} \tag{5}$$

While the PVT system converts part of the solar energy to electrical and thermal energy, the rest of the solar energy is lost to the surrounding by radiation ($\dot{Q}_{Rad}$) and convection ($\dot{Q}_{conv}$). Heat lost by radiation depends on the Stefan-Boltzmann constant (σ), the emissivity of the PV cell (ε_{PV}), the ambient temperature (T_a), and the surface area of the PV (A_{PV}).

$$\dot{Q}_{Rad} = \sigma\varepsilon_{PVT}A_{PV}(T_s^4 - T_a^4) \tag{6}$$

The heat lost by convection depends on the convective heat transfer coefficient (h_w) and the wind speed (v) [44].

$$\dot{Q}_{conv} = h_w A_{PV}(T_s - T_a) \tag{7a}$$

$$h_w = 2.8 + 3v \tag{7b}$$

The solar energy that reaches the PVT system can be expressed in terms of the rate of extracted electrical energy ($\dot{E}$), the rate of useful thermal energy and the rate of energy lost to surrounding, as shown in Eq. (8).

$$G * A_{PV} = \dot{E} + \dot{Q}_u + \left(\dot{Q}_{conv} + \dot{Q}_{Rad}\right) \tag{8}$$

The second law efficiency (η_{II}) serves as a measure of the usefulness and potential of the PVT system [45]. The overall second law efficiency is the addition of the second law efficiency of the PV cell ($\eta_{\mathrm{II},ele}$) and the second law efficiency of the thermal collector ($\eta_{\mathrm{II},th}$).

$$\eta_{\mathrm{II}} = \eta_{\mathrm{II},ele} + \eta_{\mathrm{II},th} \tag{9}$$

The rate of exergy supplied to the PVT system is the solar irradiance ($\dot{X}_{solar,in}$) whereas the rate of the recovered exergy is the electrical exergy ($\dot{X}_{ele}$) and the thermal exergy ($\dot{X}_{th}$). The second law efficiency of the PV and the thermal collector are defined as show in Eq. (10) and Eq. (11), respectively.

$$\eta_{\mathrm{II},ele} = \frac{\dot{X}_{ele}}{\dot{X}_{solar,in}} \tag{10}$$

$$\eta_{\mathrm{II},th} = \frac{\dot{X}_{th}}{\dot{X}_{solar,in}} \tag{11}$$

The rate of supplied exergy refers to the amount of solar irradiance that reaches the surface of the Earth. The most common expression is related to the Sun's temperature (T_{sun}) [46].

$$X_{solar,in} = GA_{PV}\left[1 - \frac{4}{3}\left(\frac{T_a}{T_{sun}}\right) + \frac{1}{3}\left(\frac{T_a}{T_{sun}}\right)^4\right] \tag{12}$$

The rate of recovered thermal exergy considers the portion of the heat that can be converted to work. A portion of the heat is wasted due to the disorganized nature of thermal energy [47].

$$X_{th} = \dot{m} c_p \left[(T_o - T_i) - T_a \ln \left(\frac{T_o}{T_i} \right) \right] \quad (13)$$

The rate of recovered electrical exergy is equal to the yielded electrical power. The yielded electrical energy could be fully utilized without any losses.

$$X_{ele} = \dot{E}_{ele} = \eta_{ele} G A_{PV} \quad (14)$$

All aforementioned equations are solved numerically under different operating conditions.

Chapter 4. Experimental Setup

In this chapter, the in-house PVT system components and its measuring accessories are discussed. Also, the design and fabrication process of the thermal collector is portrayed

4.1. PVT System Components

The mathematical model developed in earlier section is validated by experimental data that is collected from an in-house water-based PVT system. The PVT system consists of a polycrystalline 50 W PV module and aluminum thermal collector. The thermal collector is attached to the backside of the PV as shown in Figure 4-1. Water is circulated by a 0.5 HP pump through the inlet of the thermal collector. The water volumetric flow rate is controlled by a valve and measured by a water flow meter. The inlet and outlet water temperatures are measured by K-type thermocouples with an uncertainty of 0.15 ℃. The PV surface temperature is recorded using the Fluke Ti200 IR camera. Validating the zero-dimensional model requires recording the inlet and outlet temperatures, and the PV surface temperature at 15-minute intervals once the steady state is achieved. Data such as wind speed, solar irradiance, and ambient temperature is recorded by Davis VP2 portable weather station. Figure 4-1 shows the layout of the experiment and the instrumentation used in this study.

Blue	Cold water pipes
Red	Hot water pipes
Yellow	Solar irradiance

	Item Name
1	Water tank
2	Water pump
3	Valve
4	Flow meter
5	Weather Station
6	K-thermocouple
7	Pressure Gauge
8	Battery and control unit
9	Multi-meter
10	Thermal collector
11	IR camera
12	PV module

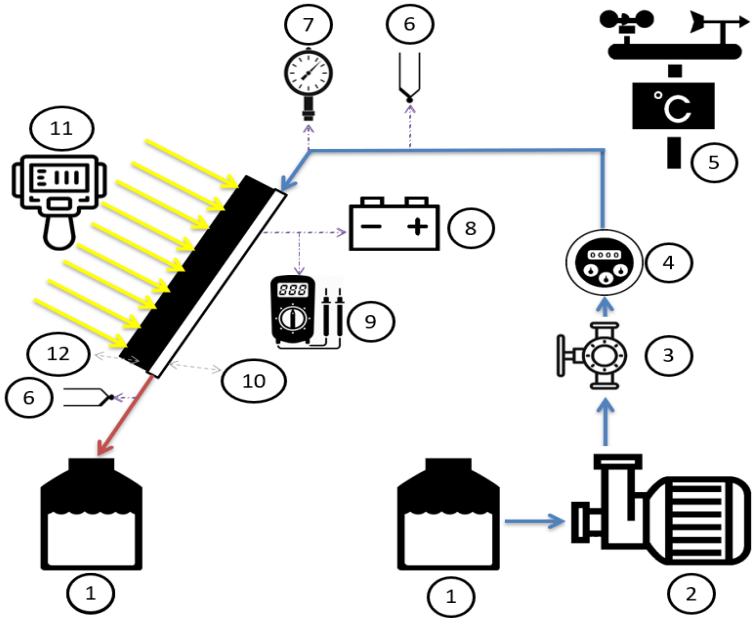

Figure 4-1: Schematic of the PVT experimental setup

4.2. Design of In-house Thermal Collector

The design of the thermal collector is based on the study conducted by Siddiqui [22] in which the double serpentine series-parallel heat sink has shown low PV surface temperature and an appropriate uniform temperature distribution. The heat sink is manufactured from aluminum plate and 10 copper pipes which are force fitted in the machined aluminum plate, as seen in Figure 4-2. The dimensions of the aluminum plate are 491 mm long, 652 mm wide, and 30 mm thick. Groove milling is performed to produce 10-mm grooves, in which the copper pipes are press fitted. The copper pipes are of 9 mm inner hydraulic diameter. The surfaces of the copper pipes are flattened to maintain proper contact area between the thermal collector and the rear side of the PV panel. The thermal collector is attached to the PV cell with the aid of thermal paste and bolts.

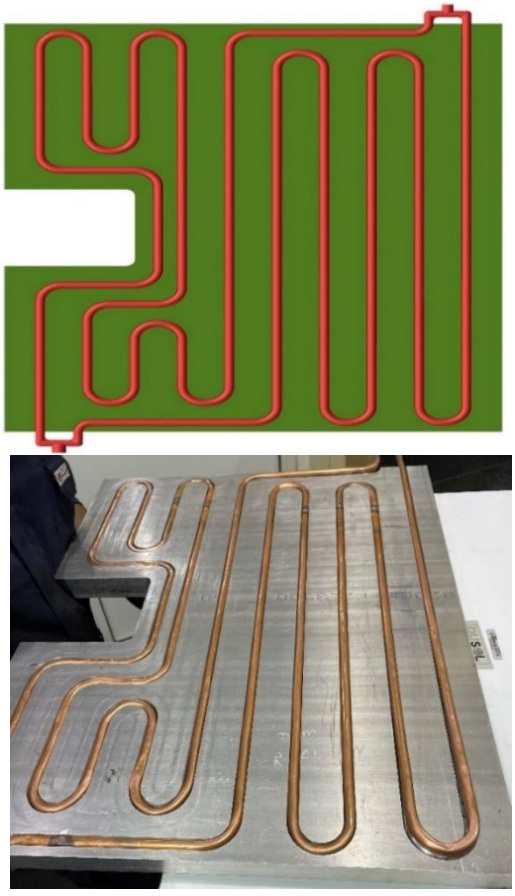

Figure 4-2: Design and implementation of the double serpentine series-parallel TC

Chapter 5. Results and Analysis

In this chapter, we validate the mathematical zero-dimensional model by comparing experimental data such as the difference in temperature between inlet and outlet as well as the surface temperature to the corresponding numerical predicted outcome. Using the experimentally validated mathematical model, parametric studies are performed to optimize the operational parameters and improve the performance of the system.

5.1. Validation of the Zero-dimensional Model

Performance of the water-based PVT system is a function of the thermal collector water inlet and outlet conditions and surface temperature of the PV cell. The difference between the thermal collector inlet and outlet temperatures determines the extracted thermal energy and the recovered thermal exergy. The electrical efficiency increases when the PV surface temperature is maintained at around room temperature [11]. Experimental data is collected from the in-house water-based PVT system and the zero-dimensional model is validated accordingly. Validity of the zero-dimension model is demonstrated in Figures 5-1 and 5-2. In the experimental part of this study, the difference between the thermal collector inlet and outlet water temperatures, the surface temperature of the PV, the wind speed, and the ambient temperature are collected at different solar irradiance levels. This data is collected for water flow rate of $0.0235\ \mathrm{kg/s}$ on different days. Over the same period of time, the recorded wind speed has varied between 1.6 and $9.6\ \mathrm{m/s}$, while the ambient temperature has varied between 24.3 and $30.0\ ℃$. The difference between the thermal collector inlet and outlet water temperatures is deduced numerically from the model and is compared to the experimental data, as shown in Figure 5-1. The zero-dimensional model is fed with the experimental data of each case as well as the PV thermal and physical parameters to estimate the change in temperature of the specified case. For instance, at solar irradiance of $292\ \mathrm{W/m^2}$, the experimental outlet water temperature is measured as $25.7\ ℃$ whereas the model outlet temperature is estimated as $25.6\ ℃$. The experimental and numerical trends are in agreement with an average error of $0.13\ ℃$. The numerical data has a coefficient of determination of $0.9321\ ℃$, which is indicative of the success of the model in predicting the difference between the thermal collector inlet and outlet water temperatures. Moreover, the result in Figure 8 shows that the difference between the thermal collector inlet and outlet water temperatures increases at higher solar

irradiance. This implies that the thermal performance of the PVT system is enhanced at high solar irradiance values.

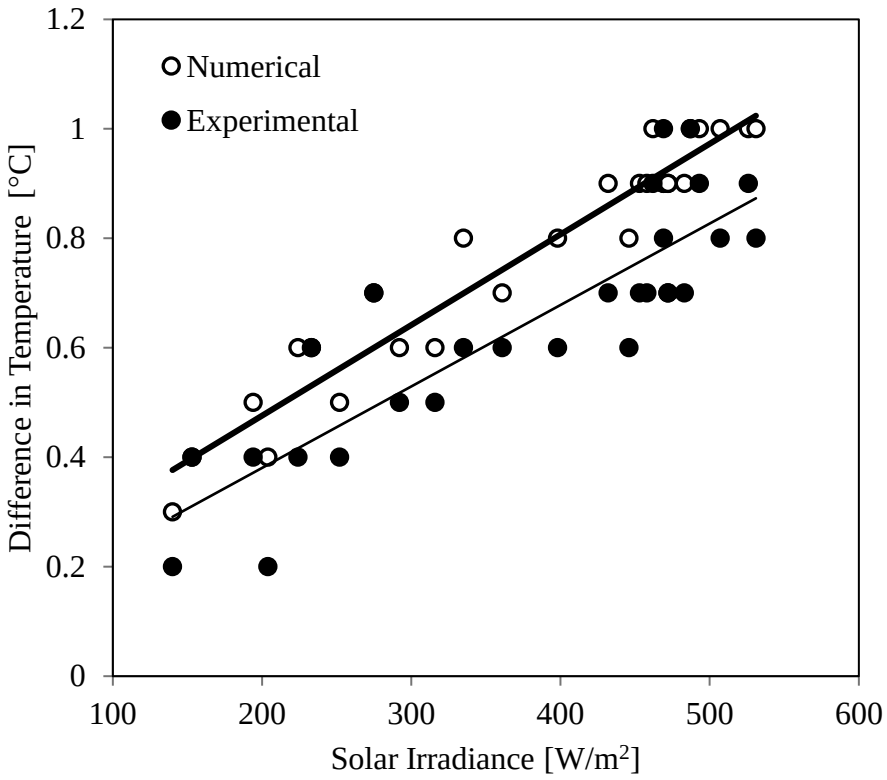

Figure 5-1: The difference in temperature between the TC inlet and outlet flow as a function of the solar irradiance

Also, the experimental PV surface temperature is compared to the numerical outcome, as seen in Figure 5-2. The trend of the numerical surface temperature matches that of the experimental surface temperature. At low solar irradiance of $224\ \mathrm{W/m^2}$, the measured PV surface temperature is $28.7\ ℃$ whereas the model estimated PV surface temperature is $27\ ℃$. Increasing the solar irradiance to $472\ \mathrm{W/m^2}$ results in an increase in the measured PV surface temperature to a value of $34.1\ ℃$ and the model estimated PV surface temperature to $31.3\ ℃$. The PV surface temperature is directly proportional to the intensity of the incident solar irradiance. The numerical model has an average error of $1.80\ ℃$ in estimating the PV surface temperature. Also, the numerical data has a low coefficient of determination of $0.6325\ ℃$. This low value of the root mean square deviation is attributed to the quasi-steady state assumption and the omission of the spatial resolution in the model.

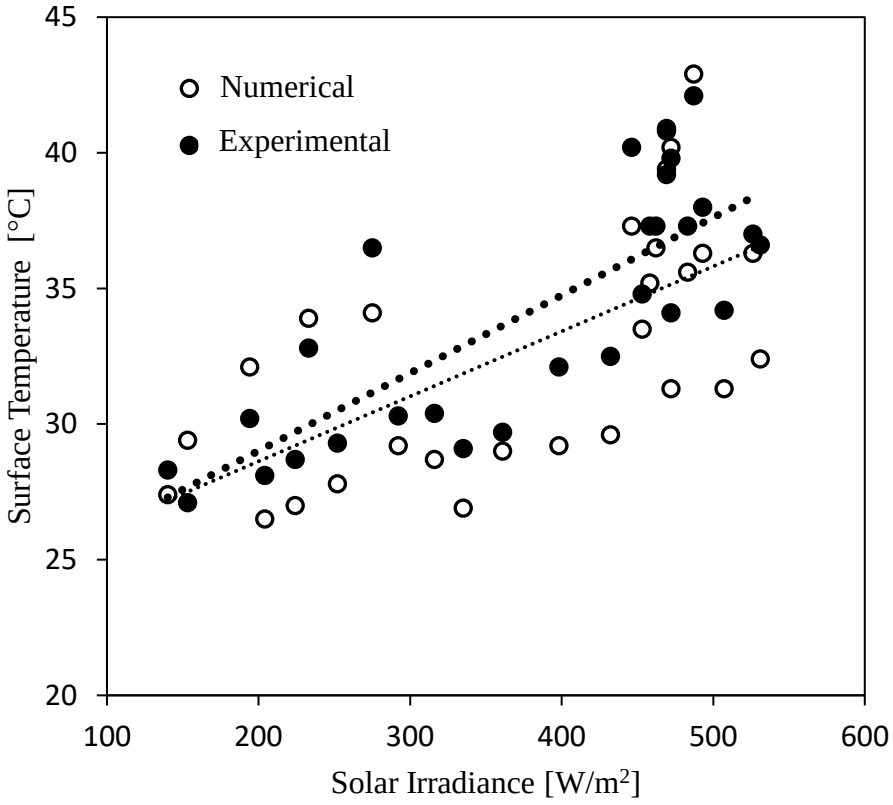

Figure 5-2: The PV surface temperature as a function of the solar irradiance

5.2. Parametric Study

Utilizing the experimental data, the weather conditions, and the physical and thermal properties, the thermal collector overall heat transfer coefficient, U_{avg}, is calculated from the zero-dimensional model. For given experimental layout, the overall heat transfer coefficient is calculated as $27.81\ \mathrm{W/(m \cdot K)}$. The low value of the overall heat transfer coefficient is mainly attributed to the high contact thermal resistance between the copper pipes, the aluminum plate and the PV module. Utilizing the zero-dimensional model, the impact of water mass flow rate on the PVT system is shown in Figure 5-3. The results in the figure are produced for an overall heat transfer of $27.81\ \mathrm{W/(m \cdot K)}$, solar irradiance of $600\ \mathrm{W/m^2}$, inlet temperature of 26.0 ℃, ambient temperature of 25.0 ℃, and thermal and physical properties listed in Table 3-1. Figure 10a shows that increasing the water mass flow rate drops the PV surface temperature until an asymptotic value at mass flow rate (0.01 kg/s). The asymptote outlet temperature approaches to the inlet temperature at high flow rates, while the surface temperature reaches a value higher than the inlet temperature due to the thermal resistance between the surface and the water. Consequently, the forced water flow at a

high volumetric flow rate has a relatively low outlet temperature as the heat removal rate from the PV declines with the increasing water mass flow rate. The lowest outlet temperature of 26.1 ℃ and the lowest PV surface temperature of 36.0 ℃ are achieved at mass flow rates above 0.01 kg/s. For the setup described in this paper, exceeding the mass flow rate values beyond 0.01 kg/s do not significantly increase thermal efficiency, electrical efficiency, and overall efficiency, as portrayed by Figure 5-3b. The reduced surface temperature implies that the electrical efficiency increases from 12.63% to 13.23%. Increasing the mass flow rate generates more hot water and that is reflected by the high thermal efficiency of 44.87%. However, the quality of this water is low and that is reflected by the exergy analysis portrayed in Figure 5-3c. The second law efficiency of the thermal collector peaks at 0.91%, at a mass flow rate of 0.0006 kg/s. This implies that the hot water has the highest available energy to be exploited and utilized in engineering applications. The second law efficiency of the PV increases by 0.64%, from 13.53% to 14.17%, as the mass flow rate is increased. This trend concludes that the first and second law electrical efficiencies are inversely proportional to the PV surface temperature. The overall second law efficiency also peaks at 0.0006 kg/s, which concludes that the optimal mass flow rate for this application is from 0.0006 kg/s to 0.003 kg/s. The performance of the PVT is affected by the wind speed, as shown in Figure 5-4. Using the optimized mass flow rate of 0.001 kg/s, the wind speed varied between 0 m/s and 15 m/s, while the other operational and weather parameters remain constant. Increasing the wind speeds decrease the surface temperature and the outlet temperature, as depicted in Figure 5-4a. The heat lost through convection increases significantly resulting in a lowered surface temperature and a diminished ability in extracting heat through the water flow. Consequently, Figure 5-4b shows that the thermal and the overall efficiencies decrease, whereas the electrical efficiency increases from 12.4% to 13.4%. From energy analysis, the highest thermal efficiency of 50.6% is calculated at the lowest wind speed of 0 m/s, ensuring that the convective and radiative losses are minimal. However, the highest electrical efficiency of 13.4% is achieved at the highest wind speed of 15 m/s and the lowest PV surface temperature of 33℃. These trends are somewhat similar for the exergy analysis, in which the second law efficiency of the TC varies inversely with the wind speed. On the other hand, the second law efficiency of the PV varies directly with the wind speed. This could be attributed to the decreasing rate of heat extraction

as the wind speed increases. In short, higher wind speed allows better cooling of the PVT system which improves the PV electric power conversion, but it reduces the thermal energy collected by the thermal collector. Figure 5-3 shows the effect of mass flow rate on the outlet temperature, the PV surface temperature, the overall efficiency and the overall second law efficiency.

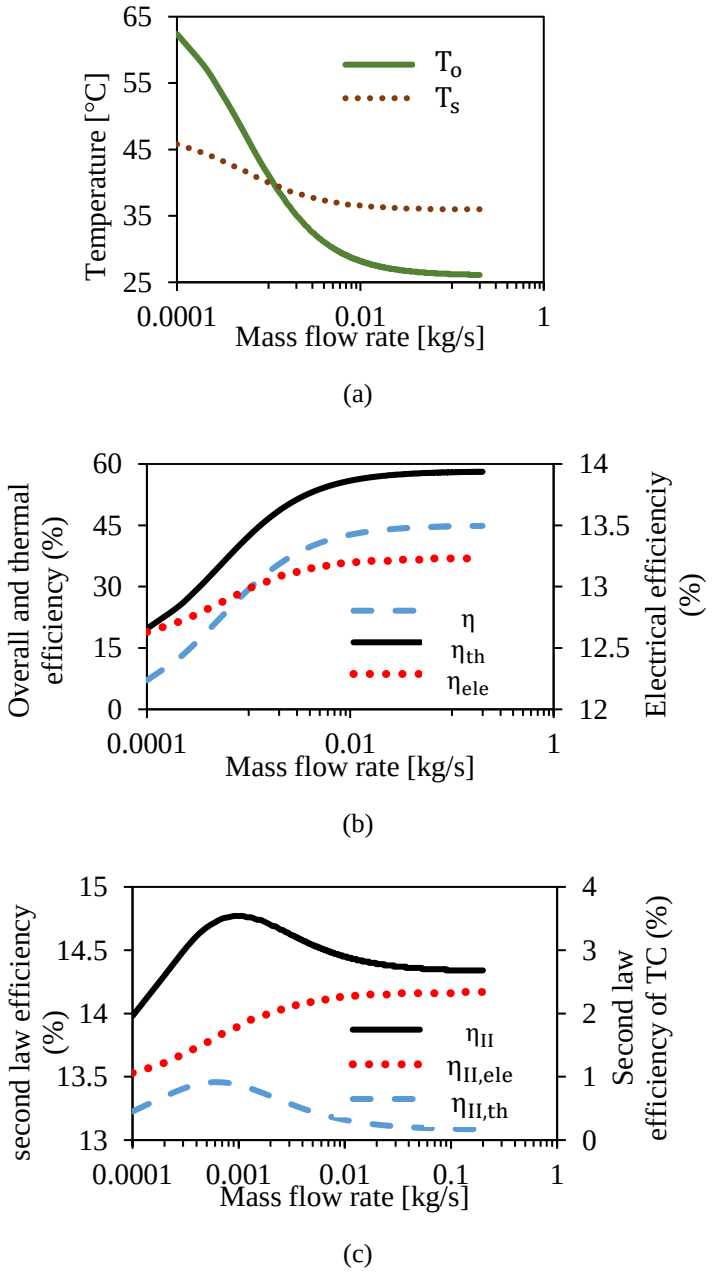

Figure 5-3: The effect of mass flow rate on (a) Outlet water temperature and PV surface temperature (b) Overall efficiency (c) Overall second law efficiency

Similarly, Figure 5-4 shows the impact of wind speed on the PVT performance.

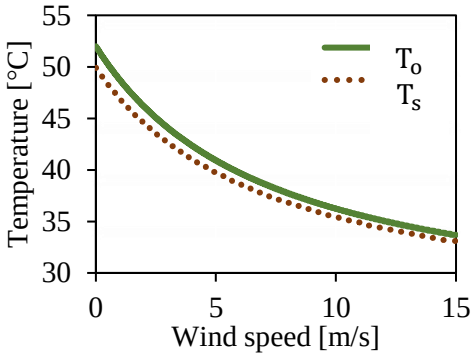

(a)

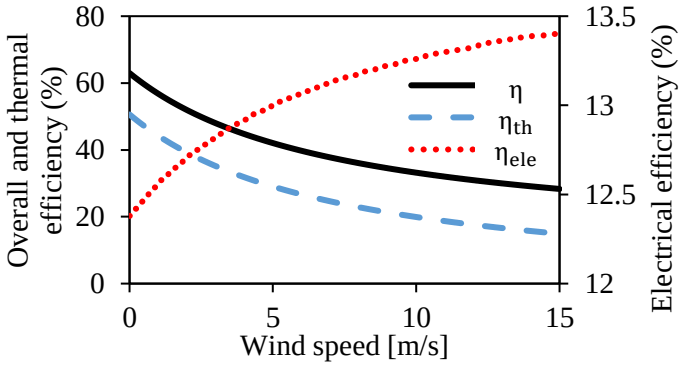

(b)

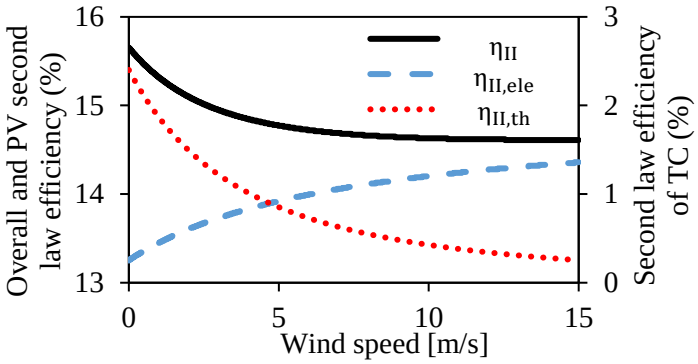

(c)

Figure 5-4: The effect of wind speed on (a) Outlet water temperature and PV surface temperature (b) Overall efficiency (c) Overall second law efficiency

The impact of inlet temperature on PVT performance is illustrated in Figure 5-5. Using a mass flow rate of 0.001 kg/s, the inlet temperature is varied with the weather conditions, while thermal properties, and physical characteristics remain constant. Increasing the inlet temperature from 15°C to 47.6°C increases the surface and outlet water temperatures until they reach to an equilibrium, as shown in Figure 5-5a. The inlet water with low thermal content cools down the PV cell, which in turn leads to a relatively low surface temperature and a large difference between the outlet and inlet

water temperatures. Comparatively, the inlet water with high thermal content does not cool the PV cell properly, and the corresponding difference in temperature between the outlet and inlet waters is minimal. In Figure 5-5a, when the inlet temperature is $47.6°C$, no heat is extracted by the water in the pipes since the produced electricity, and the heat lost through convection and radiation are equal to the solar irradiance received by PVT system. This implies that the thermal efficiency reaches to 0%, whereas the electrical efficiency decreases from 13.2% to 12.5%, as observed in Figure 5-5b. Energy analysis suggests the lowest inlet water temperature to have the highest possible overall efficiency. From the exergy analysis shown in Figure 5-5c, the second law PV efficiency remains the highest, 14.2%, at the lowest inlet water temperature. However, a low inlet water temperature yields a low quality outlet water. Therefore, having the inlet water temperature range between $22.5°C$ and $27.5°C$ ensures the optimal performance of the PVT system. The ambient temperature $25°C$ lies within the optimal range of inlet water temperature. Having the inlet water temperatures lower than the ambient temperature results in entropy generation due to rapid heating of water. Accordingly, the water heats to a temperature that yields a lower exergy. In contrast, a water flow with an inlet temperature higher than the ambient temperature does not heat up significantly, which results in a lower potential to do work. Regardless of the inlet temperature, the second law efficiency of the TC remains relatively low. However, it is observed that an inlet water flow close to the ambient temperature yields the highest available energy. In Figure 5-6, the effect of ambient temperature and solar irradiance on the performance of the PVT system is studied in 3 scenarios that are common to UAE's weather conditions. Namely, (a) the ambient temperature is $20\ °C$ and the solar irradiance is $400\ W/m^2$, (b) the ambient temperature is $30\ °C$ and the solar irradiance is $600\ W/m^2$, and (c) the ambient temperature is $40\ °C$ and the solar irradiance is $800\ W/m^2$. Increasing the ambient temperature decreases the second law efficiencies of both the PV and the overall PVT system. At the optimum mass flow rate of $0.001\ kg/s$, the second law efficiency of the PV is highest at the lowest inlet water temperature of $15\ °C$ along with the lowest ambient temperature of $20\ °C$, as shown in Figure 5-6a. This behavior is expected for the PV since low inlet water and ambient temperatures ensure low surface temperature, which is favorable to electricity production.

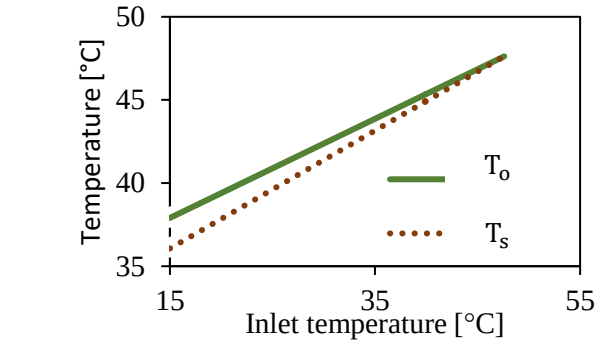

(a)

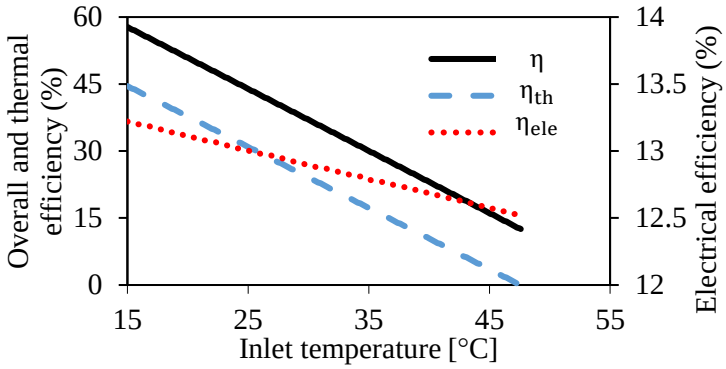

(b)

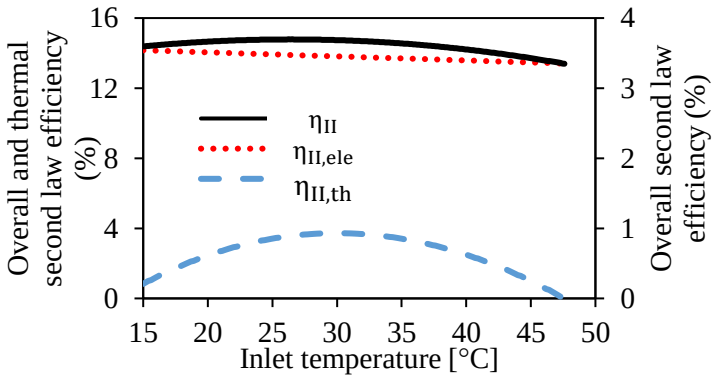

(c)

Figure 5-5: The effect of inlet water temperature on (a) Outlet water temperature and PV surface temperature (b) Overall efficiency (c) Overall second law efficiency

The overall PVT second law efficiency is the highest at the lowest ambient temperature and at an inlet water temperature that is in the vicinity of the ambient temperature, as shown in Figure 5-6b. The overall PVT second law efficiency peaks at 15.2% as the inlet water and ambient temperatures, and solar irradiance are $21.5\ °C, 20\ °C,$ and $400\ W/m^2$, respectively. In Figure 5-6b, the parabolic trends are attributed to the significant exergy destructed at low and high inlet water temperatures.

The trends shown in Figure 5-6 conclude that the overall performance of the PVT is optimum in weather conditions with high solar irradiance yet reasonable ambient temperature. While the GCC countries receive an abundance of solar radiation, the hot climate limits the efficiency and the performance of the implemented PVT systems.

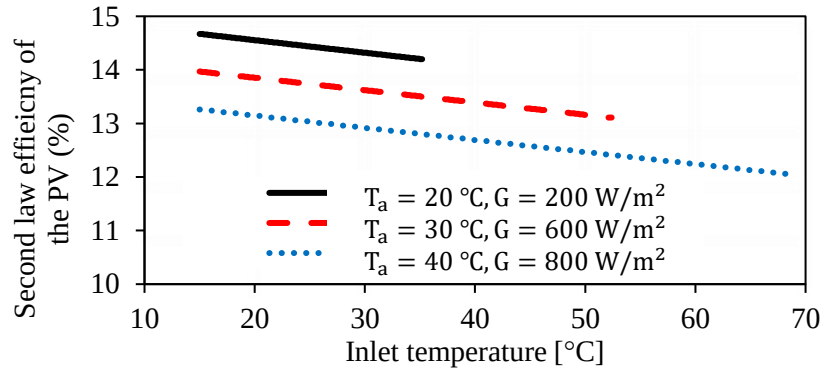

(a)

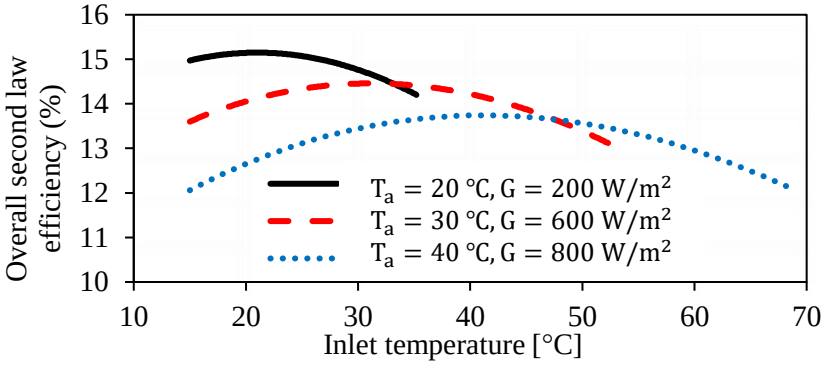

(b)

Figure 5-6: (a) Second law efficiency of the PV (b) Overall second law efficiency of the PVT system as a function of the operational parameters at mass flow rate of 0.001 kg/s

Figure 5-7 shows the effect of varying both the mass flow rate and the inlet water temperature on the performance of the PVT, when the ambient temperature is 30 °C and the solar irradiance is 600 W/m^2. As seen in Figure 5-7a, the second law efficiency of the PV decreases as the inlet water temperature rises, regardless of the mass flow rate. Using the optimized mass flow rate of 0.001 kg/s, the second law efficiency of the PV is maximized at 13.9% when inlet temperature 18.1 °C. However, the overall second law efficiency trends are parabolic showing that exergy is maximized at a specified range of inlet water temperatures. For mass flow rate of 0.0003 kg/s, the peak performance is at inlet water temperature ranging between 13.0 °C and 19.0 °C, as seen in Figure 5-7b. The water extracts low quantities of heat at high inlet

temperatures, whereas the thermal quality of the heated water is low at low inlet temperatures. PVT systems that utilize mass flow rates of $0.001\ kg/s$ and $0.05\ kg/s$ peak at median inlet water temperatures of $31.5\ ℃$ and $39\ ℃$, respectively. Increasing the mass flow rate requires the usage of an elevated inlet water temperature, due to the fact that low inlet water temperature will yield low thermal quality water. With the inlet water temperatures above $52.3\ ℃$, the water does not heat up and the operation of the PVT system is not justifiable. The trends shown in Figure 5-7 conclude that the optimal performance of the PVT system is achieved when the elevated inlet water temperatures are used at high mass flow rates, whereas the low inlet water temperatures are used at low mass flow rates.

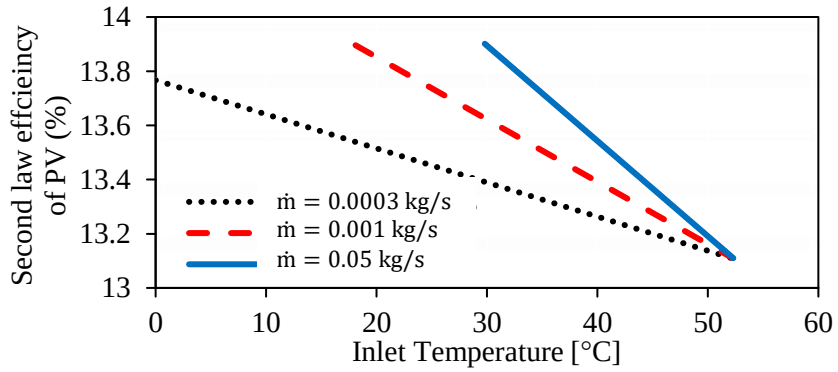

(a)

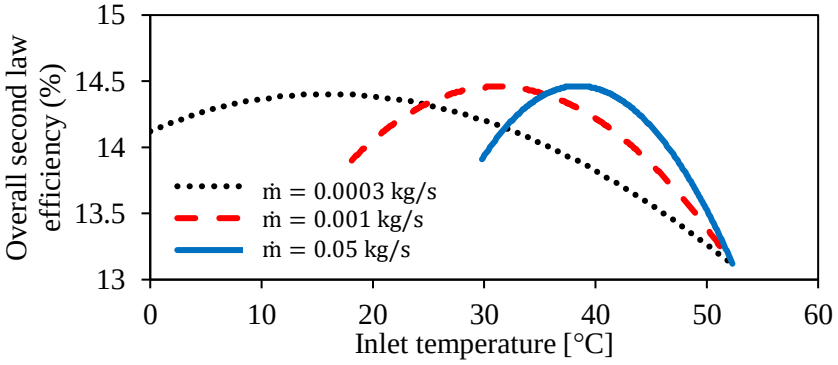

(b)

Figure 5-7: (a) Second law efficiency of the PV (b) Overall second law efficiency of the PVT system as a function of the operational parameters at ambient temperature of 30 °C and solar irradiance of 600 W/m^2

Chapter 6. Conclusion and Future Work

6.1. Summary

This thesis validates the zero-dimensional model with the experimental data obtained from an in-house PVT system and weather station. Two significant operational parameters, namely the difference between inlet and outlet water temperatures as well as the PV surface temperature, matched the numerically acquired estimations with reasonable accuracy. In accordance with the experimental data, the difference between the inlet and outlet water temperatures increased at higher solar irradiances. Likewise, the zero-dimensional model estimated an increase in PV surface temperature as the solar irradiation intensifies. The zero-dimensional model is a reliable method in computing the overall heat transfer coefficient. Upon supplying the model with all operational parameters, such as the inlet and outlet water temperatures, the PV surface temperature, the mass flow rate, as well as the thermo-physical properties of the PVT system and the weather conditions at the site of the experiment, the overall heat transfer coefficient is computed as 24.7 W/(m·K). The low overall heat transfer coefficient is attributed to the inherently high thermal resistance in the design of the PVT system. Extending the usage of the zero-dimensional model, performance parameters such as the overall first and second law efficiencies are determined as operational parameters are varied. The optimal mass flow rate of 0.001 kg/s ensures the highest available energy, as utilizing a relatively low mass flow rate does not yield enough thermal energy removal, whereas relatively high mass flow yields low available energy removal. Upon choosing the optimal inlet water temperature that optimizes the performance of the PVT system, the energy analysis gives misleading results, whereas the exergy analysis gives a more accurate conclusion. While a low inlet water temperature, 15 ℃, ensures high electrical efficiency and high second law efficiency of the PV, the second law efficiency of the TC is extremely low at such temperature since the yielded water is at low thermal quality. The study shows that an inlet water temperature that is close to the ambient temperature gives the highest overall second law efficiency. Relative to the ambient temperature, high PVT overall second law efficiency is achieved for the cases of low mass flow rate flow, with a relatively low inlet water temperature, as well as the case of high mass flow rate flow with a relatively

high inlet water temperature. Finally, the study concluded that the performance of the PVT system is optimal in relatively cold regions that receive high solar radiation.

6.2. Future Work

The zero-dimensional model is a strong tool in studying different operating liquids for the PVT system. Future work could include studying the effects of nanofluids, phase-change materials, and organic compounds on the performance of the PVT system using the proposed zero-dimensional model. Also, the zero-dimensional could be extended to predict the performance of various PVT systems such as: Air-cooled PVT system, concentrating PVT systems, and Fresnel lens integrated PVT systems. Apart from the energy and exergy analysis of the PVT system, research related to the cost analysis and life cycle assessment of such systems would enrich the available literature.

References

[1] N. W. Alnaser and W. E. Alnaser, "The impact of the rise of using solar energy in GCC countries," *Renew. Energy Environ. Sustain.*, vol. 4, no. 7, pp. 1-11, 2019.

[2] T. T. Chow, W. He, A. L. S. Chan, K. F. Fong, Z. Lin, and J. Ji, "Computer modeling and experimental validation of a building-integrated photovoltaic and water heating system," *Applied Thermal Engineering*, vol. 28, no. 11, pp. 1356-1364, 2008/08/01/ 2008, doi: https://doi.org/10.1016/j.applthermaleng.2007.10.007.

[3] E. Radziemska, "Performance Analysis of a Photovoltaic-Thermal Integrated System," *International Journal of Photoenergy*, vol. 2009, p. 732093, 2009, doi: 10.1155/2009/732093.

[4] A. Fudholi, K. Sopian, M. H. Yazdi, M. H. Ruslan, M. Gabbasa, and H. A. Kazem, "Performance analysis of solar drying system for red chili," *Solar Energy*, vol. 99, pp. 47-54, 2014, doi: https://doi.org/10.1016/j.solener.2013.10.019.

[5] Z. Han, K. Liu, G. Li, X. Zhao, and S. Shittu, "Electrical and thermal performance comparison between PVT-ST and PV-ST systems," *Energy*, vol. 237, p. 121589, 2021, doi: https://doi.org/10.1016/j.energy.2021.121589.

[6] S. Al Naqbi, I. Tsai, and T. Mezher, "Market design for successful implementation of UAE 2050 energy strategy," *Renewable and Sustainable Energy Reviews*, vol. 116, p. 109429, 2019, doi: https://doi.org/10.1016/j.rser.2019.109429.

[7] N. A, G. H, and B. M, "Experimental Analysis PVP Coated Silver Nanofluid Properties for Application in Photovoltaic/Thermal (PVT) Collectors," *Journal of Model Based Research*, vol. 1, no. 3, pp. 28-40, 2020, doi: https://doi.org/10.14302/issn.2643-2811.jmbr-20-3476.

[8] P. Dwivedi, K. Sudhakar, A. Soni, E. Solomin, and K. Irina, "Advanced cooling techniques of P.V. modules: A state of art," *Case Studies in Thermal Engineering*, vol. 21, p. 100674, 2020, doi: 10.1016/j.csite.2020.100674.

[9] D. Sato and N. Yamada, "Review of photovoltaic module cooling methods and performance evaluation of the radiative cooling method," *Renewable and Sustainable Energy Reviews*, vol. 104, pp. 151-166, 2019, doi: https://doi.org/10.1016/j.rser.2018.12.051.

[10] H. G. Teo, P. S. Lee, and M. N. A. Hawlader, "An active cooling system for photovoltaic modules," *Applied Energy*, vol. 90, no. 1, pp. 309-315, 2012, doi: https://doi.org/10.1016/j.apenergy.2011.01.017.

[11] E. Radziemska, "The effect of temperature on the power drop in crystalline silicon solar cells," *Renewable Energy*, vol. 28, no. 1, pp. 1-12, 2003, doi: https://doi.org/10.1016/S0960-1481(02)00015-0.

[12] D. Quansah, "Investigation of Solar Photovoltaic-Thermal (PVT) and Solar Photovoltaic (PV) Performance: A Case Study in Ghana," *Energies*, vol. 13, no. 11, p. 2701, 2020, doi: 10.3390/en13112701.

[13] J.-H. Kim and J.-T. Kim, "Comparison of Electrical and Thermal Performances of Glazed and Unglazed PVT Collectors," *International Journal of Photoenergy*, vol. 2012, pp. 1-7, 2012, doi: 10.1155/2012/957847.

[14] T. Fujisawa and T. Tani, "Annual exergy evaluation on photovoltaic-thermal hybrid collector," *Solar Energy Materials and Solar Cells*, vol. 47, no. 1, pp. 135-148, 1997, doi: https://doi.org/10.1016/S0927-0248(97)00034-2.

[15] A. Kazemian, M. Hosseinzadeh, M. Sardarabadi, and M. Passandideh-Fard, "Effect of glass cover and working fluid on the performance of photovoltaic thermal (PVT) system: An experimental study," *Solar Energy*, vol. 173, pp. 1002-1010, 2018, doi: https://doi.org/10.1016/j.solener.2018.07.051.

[16] Y. Tripanagnostopoulos, T. Nousia, M. Souliotis, and P. Yianoulis, "Hybrid photovoltaic/thermal solar systems," *Solar Energy*, vol. 72, no. 3, pp. 217-234, 2002, doi: https://doi.org/10.1016/S0038-092X(01)00096-2.

[17] A. Ibrahim, M. Y. Othman, M. H. Ruslan, S. Mat, and K. Sopian, "Recent advances in flat plate photovoltaic/thermal (PV/T) solar collectors," *Renewable and Sustainable Energy Reviews*, vol. 15, no. 1, pp. 352-365, 2011, doi: https://doi.org/10.1016/j.rser.2010.09.024.

[18] Y. Yu, H. Yang, J. Peng, and E. Long, "Performance comparisons of two flat-plate photovoltaic thermal collectors with different channel configurations," *Energy*, vol. 175, pp. 300-308, 2019, doi: https://doi.org/10.1016/j.energy.2019.03.054.

[19] S. K. Verma, K. Sharma, N. K. Gupta, P. Soni, and N. Upadhyay, "Performance comparison of innovative spiral shaped solar collector design with conventional flat plate solar collector," *Energy*, vol. 194, p. 116853, 2020, doi: https://doi.org/10.1016/j.energy.2019.116853.

[20] D. Del Col, A. Padovan, M. Bortolato, M. Dai Prè, and E. Zambolin, "Thermal performance of flat plate solar collectors with sheet-and-tube and roll-bond absorbers," *Energy*, vol. 58, pp. 258-269, 2013, doi: https://doi.org/10.1016/j.energy.2013.05.058.

[21] I. Visa *et al.*, "Design and experimental optimisation of a novel flat plate solar thermal collector with trapezoidal shape for facades integration," *Applied Thermal Engineering*, vol. 90, pp. 432-443, 2015, doi: https://doi.org/10.1016/j.applthermaleng.2015.06.026.

[22] M. U. Siddiqui, O. K. Siddiqui, A. Al-Sarkhi, A. F. M. Arif, and S. M. Zubair, "A novel heat exchanger design procedure for photovoltaic panel cooling application: An analytical and experimental evaluation," *Applied Energy*, vol. 239, pp. 41-56, 2019, doi: https://doi.org/10.1016/j.apenergy.2019.01.203.

[23] H. A. Kazem, A. H. A. Al-Waeli, M. T. Chaichan, K. H. Al-Waeli, A. B. Al-Aasam, and K. Sopian, "Evaluation and comparison of different flow configurations PVT systems in Oman: A numerical and experimental investigation," *Solar Energy*, vol. 208, pp. 58-88, 2020, doi: https://doi.org/10.1016/j.solener.2020.07.078.

[24] A. Ibrahim, M. Y. Othman, M. H. Ruslan, S. Mat, A. Zaharim, and K. Sopian, "Experimental studies on water based photovoltaic thermal collector (PVT)," in *Proceedings of the 9th WSEAS international conference on System science and simulation in engineering*, 2010, pp. 439-443.

[25] Y. Pang, Q. Zhang, Y. Cui, L. Zhang, H. Yu, X. Zhang, and Y. Zhang, "Numerical simulation and experimental validation of a photovoltaic/thermal system based on a roll-bond aluminum collector," *Energy*, vol. 187, p. 115990, 2019, doi: https://doi.org/10.1016/j.energy.2019.115990.

[26] A. Ibrahim, M. Y. Othman, M. H. Ruslan, M. Alghoul, M. A. Yahya, A. Zaharim, and K. Sopian, "Performance of photovoltaic thermal collector (PVT)

with different absorbers design," *WSEAS Transactions on Environment and Development*, vol. 5, pp. 321-330, 2009.

[27] H. Fayaz, N. A. Rahim, M. Hasanuzzaman, A. Rivai, and R. Nasrin, "Numerical and outdoor real time experimental investigation of performance of PCM based PVT system," *Solar Energy*, vol. 179, pp. 135-150, 2019, doi: https://doi.org/10.1016/j.solener.2018.12.057.

[28] H. A. Zondag, D. W. de Vries, W. G. J. van Helden, R. J. C. van Zolingen, and A. A. van Steenhoven, "The thermal and electrical yield of a PV-thermal collector," *Solar Energy*, vol. 72, no. 2, pp. 113-128, 2002, doi: https://doi.org/10.1016/S0038-092X(01)00094-9.

[29] H. Pierrick, M. Christophe, G. Leon, and D. Patrick, "Dynamic numerical model of a high efficiency PV–T collector integrated into a domestic hot water system," *Solar Energy*, vol. 111, pp. 68-81, 2015, doi: https://doi.org/10.1016/j.solener.2014.10.031.

[30] I. Guarracino, A. Mellor, N. J. Ekins-Daukes, and C. N. Markides, "Dynamic coupled thermal-and-electrical modelling of sheet-and-tube hybrid photovoltaic/thermal (PVT) collectors," *Applied Thermal Engineering*, vol. 101, pp. 778-795, 2016, doi: https://doi.org/10.1016/j.applthermaleng.2016.02.056.

[31] A. M. A. Soliman, H. Hassan, M. Ahmed, and S. Ookawara, "A 3d model of the effect of using heat spreader on the performance of photovoltaic panel (PV)," *Mathematics and Computers in Simulation*, vol. 167, pp. 78-91, 2020, doi: https://doi.org/10.1016/j.matcom.2018.05.011.

[32] S. Sami, "Modeling and Simulation of a Novel Combined Solar Photovoltaic-Thermal Panel and Heat Pump Hybrid System," *Clean Technologies*, vol. 1, no. 1, pp. 89-113, 2019, doi: 10.3390/cleantechnol1010007.

[33] S. Dubey and G. N. Tiwari, "Thermal modeling of a combined system of photovoltaic thermal (PV/T) solar water heater," *Solar Energy*, vol. 82, no. 7, pp. 602-612, 2008, doi: https://doi.org/10.1016/j.solener.2008.02.005.

[34] J. Ji, H. He, T. Chow, G. Pei, W. He, and K. Liu, "Distributed dynamic modeling and experimental study of PV evaporator in a PV/T solar-assisted heat pump," *International Journal of Heat and Mass Transfer*, vol. 52, no. 5, pp. 1365-1373, 2009, doi: https://doi.org/10.1016/j.ijheatmasstransfer.2008.08.017.

[35] A. Tiwari and M. S. Sodha, "Performance evaluation of solar PV/T system: An experimental validation," *Solar Energy*, vol. 80, no. 7, pp. 751-759, 2006, doi: https://doi.org/10.1016/j.solener.2005.07.006.

[36] H. Bahaidarah, A. Subhan, P. Gandhidasan, and S. Rehman, "Performance evaluation of a PV (photovoltaic) module by back surface water cooling for hot climatic conditions," *Energy*, vol. 59, pp. 445-453, 2013, doi: https://doi.org/10.1016/j.energy.2013.07.050.

[37] G. Evola and L. Marletta, "Exergy and thermoeconomic optimization of a water-cooled glazed hybrid photovoltaic/thermal (PVT) collector," *Solar Energy*, vol. 107, pp. 12-25, 2014, doi: https://doi.org/10.1016/j.solener.2014.05.041.

[38] A. Abdulalah, S. Misha, N. Tamaldin, M. A. Mohd Rosli, and F. Sachit, "Theoretical study and indoor experimental validation of performance of the new photovoltaic thermal solar collector (PVT) based water system," *Case Studies in Thermal Engineering*, vol. 18, p. 100595, 2020, doi: 10.1016/j.csite.2020.100595.

[39] H. Fayaz, R. Nasrin, N. A. Rahim, and M. Hasanuzzaman, "Energy and exergy analysis of the PVT system: Effect of nanofluid flow rate," *Solar Energy*, vol. 169, pp. 217-230, 2018/07/15/ 2018, doi: https://doi.org/10.1016/j.solener.2018.05.004.
[40] Massachusetts Department of Energy Resources, "Ground Mounted Solar Photovoltaic Systems,". Internet: solar-QA-revised report 6_1_15 (mass.gov), 2015, [May. 10, 2021].
[41] M. Alam and M. Khan, "Fundamentals of PV Efficiency Interpreted by a Two-Level Model," *American Journal of Physics*, vol. 81, pp. 312-316, 2012, doi: 10.1119/1.4812594.
[42] I. Guarracino, J. Freeman, A. Ramos, S. A. Kalogirou, N. J. Ekins-Daukes, and C. N. Markides, "Systematic testing of hybrid PV-thermal (PVT) solar collectors in steady-state and dynamic outdoor conditions," *Applied Energy*, vol. 240, pp. 1014-1030, 2019, doi: https://doi.org/10.1016/j.apenergy.2018.12.049.
[43] Y. Cengel and A. Ghajjar, *Heat and Mass Transfer: Fundamentals and Applications*, New York: McGraw-Hill Professional, 2014, pp. 649-672.
[44] J. Watmuff, W. Charters, and D. Proctor, "Solar and wind induced external coefficients - Solar collectors," *Cooperation Mediterraneenne pour l'Energie Solaire*, vol. 1, p. 56, 1977.
[45] Y. Cengel and M. Boles, *Thermodynamics: An Engineering Approach*, Boston: McGraw-Hill Higher Education, 2014, pp. 275-312.
[46] R. Petela, "Exergy of Heat Radiation," *Journal of Heat Transfer*, vol. 86, no. 2, pp. 187-192, 1964, doi: 10.1115/1.3687092.
[47] A. Hepbasli, "A key review on exergetic analysis and assessment of renewable energy resources for a sustainable future," *Renewable and Sustainable Energy Reviews*, vol. 12, no. 3, pp. 593-661, 2008, doi: https://doi.org/10.1016/j.rser.2006.10.001.

Appendix A

Table A-1: Electrical specifications of PV module (STC)

Nominal power	49 W
Open-circuit voltage	22.12 V
Short-circuit current	2.983 A
Voltage at maximum power	18.37 V
Maximum power current	2.667 A
Efficiency module	13.9 %

Table A-2: Mechanical data of PV module

Length	535 mm
Width	670 mm
Depth	34 mm
Weight	4.7 kg

Table A-3: Properties of the thermal paste

Material type	Thermal Silicon compound
Shear strength	1.5 MPa
Thermal conductivity	>0.671 W/m. K
Solidification time	3 min

Figure A-1: Front-side of the PVT system

Figure A-2: Rear-side of the PVT system

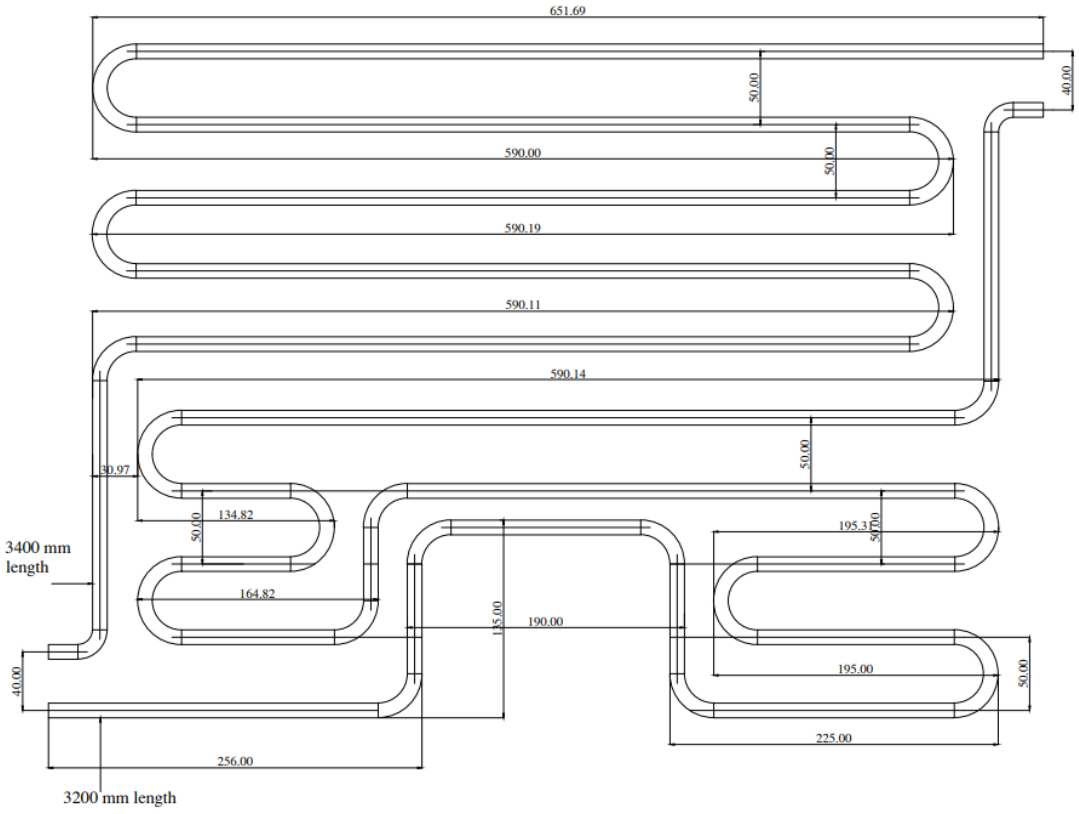

Figure A-3: Dimensions of the thermal collector

Vita

Khader M.J. Alsayegh was born in 1998, in Sharjah, United Arab Emirates. He received his primary and secondary education in Sharjah, UAE. He received his B.Sc. degree in Mechanical Engineering from the American University of Sharjah in 2020.

In September 2020, he joined the Mechanical Engineering master's program in the American University of Sharjah as a graduate teaching assistant. During his master's study, he co-authored several papers which were presented in international conferences and journals. His research interests are related to renewable energy systems, fluid and thermal systems, and artificial intelligence systems.